18th Brazilian Congress of Thermal Sciences and Engineering
November 16-20, 2020 (Online)

# ENCIT-2020-0549
# EXPERIMENTAL MEASUREMENTS OF CONVECTIVE HEAT TRANSFER COEFFICIENT AROUND A SINGLE BUNDLE IN COMPOUND CHANNEL

**Fábio Matos Kayser**[1]
fabio_mk_66@hotmail.com

**Alexandre Alencar de Melo**[2]
jucaalencarmelo@gmail.com

**Jalusa Maria da Silva Ferrari**[3]
jalusaferrari@gmail.com

**Jhon Nero Vaz Goulart**[4]
jvazgoulart@gmail.com

(1,2,3,4) Group of Experimental and Computational Mechanics — GMEC.
University of Brasilia, PO box 8114, Gama, DF, zip code: 72.444-240, Brazil

***Abstract.*** *This work aims to evaluate the experimentally the convective heat transfer coefficient around a single rod bundle. The single rod bundle is part of a compound channel that is mainly characterized by their dimensionless numbers such as the Reynolds number, and the W/D - ratio. The gap g is the distance between the rod and the upper part of the channel. During the experimental campaign the gap g was changed its width, 10 and 5 mm, yielding a W/D = 1.10 and 1.05, respectively.The dimension W is the sum of the gap, g, plus the cylinder's radius. The test section length was kept constant, 1800 mm. Special heated cell, controlled by a Minipa 3305 Power Supply, was designed.in order to keep cell`s surface heated. The temperature on the cell`s surface was acquired through a set of special thermocouples on it. Regardless the W/D test sections coherent structures, yielding periodic flow velocity patterns, were found at the gap vicinity. As regards the Nusselt number measurements was found in good agreement with previous data from another researchers.*

***Keywords:*** *Nusselt number, heated cell, compound channel, rod bundle, coherent structures, hot wire anemometry.*

## 1. INTRODUCTION

Channels with a main channel containing subchannels connected by gaps are known as compound channels (Goulart et al., 2016 and Melo et al., 2017). Flow in structures with compound channels are characterized by instabilities and values of the turbulent stresses that are not found in another simple channel (Goulart et al., 2016 and Severino, 2018, Candela et al., 2020).

Convection is a heat transfer mechanism that involves both heat transfer by conduction and by advection (fluid movement). When studying convection, it is common to use equations in the dimensionless form, considering that dimensioning factors that group together reduces the number of variables with which one works. In this respect, it ends up dimensioning *the convection heat transfer coefficient* (*h*) using the Nusselt Number. The *Nusselt Number* (*Nu*) is the ratio between heat transfer by convection and by conduction. Thus, this parameter makes it possible to verify the increase in heat transfer due to the movement of the fluid in relation to heat transfer by conduction (Guellouz and Tavoularis, 1992).

This work aims to evaluate experimentally the convective heat transfer processes in a closed compound channel. The channel is formed by a sing rod bundle, quite similar to the test section studied by Guellouz and his co-worker in 90`s. Further, is also target of this work the establishment of the relationship between the heat transfer process enhancements facing the coherent structure formation. During the experimental campaign the velocity fluctuation time-traces were acquired by means hot-wire probes. In order to attain our goals we studied two different *W/D* – ratio, 1.10 and 1.05.

## 2. EXPERIMENTAL PROCEDURE

The experiment was carried out in an acrylic rectangular, containing a centrifugal fan at the extremity, according to Figure 1. Inside the channels air at room temperature is the work fluid, whose its free stream velocity, $U_{ref}$, is controlled by a frequency inverter. The air passes through a set of screens and honeycombs before reaching the test section itself. The teste section is formed by a single rod bundle apart from the channel`s upper wall by a distance *d*. In this way both lateral subchannels are connected through the thigh gap.

Figure 1 (a) and (b) shows the lateral view and the transversal section of the channel. The total length of the channel (*LT*) is 3000 mm, the test section length (*LS*) is 1800 mm. The dimensions *L1* and *L2* are 525 mm and 475 mm, respectively. For the transversal section, *WC* = 200 mm, *HC* = 150 mm and *D* = 100 mm. In this experimente were used two gap width (*d*), 5 and 10 mm.

The velocity and spectra were gathered by the hot-wire technique. The data processing was carried out in the TSI IFA-300 hot-wire system, which can acquire signals up to 300 kHz. The calibration and the data gathering were conducted by the TermalPRO software, available by the manufacturer. It was used a single probe TSI 1201. The velocity signals were sampled at 1 kHz with a low pass filter set at 300 Hz, and digitalized by a A/D board 16 Bits.

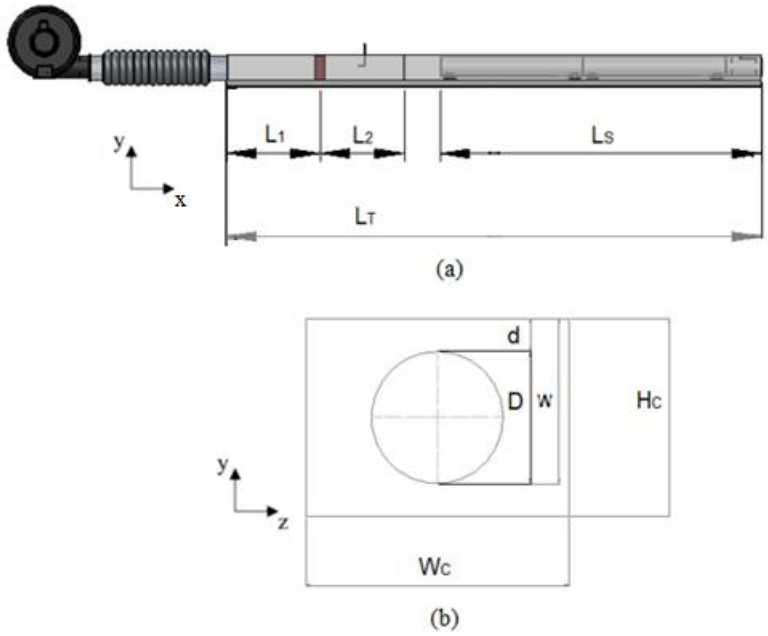


Figure 1. Channel dimensions. (a) Lateral view. (b) Transversal section.

At the end of the rod, about 200 mm upstream the channel`s outlet there is a heated cell mounted on the of the rod, as shown in Figure 2. The cell is heated by a MINIPA MPL-3305M electrical source and is completely insulated. The cell can be turned around the rod, assuming different angular position. In order to acquire the temperatures, five thermocouples were placed in the heated cell and in the adjacent region. According to the indications seen in the Figure 2, the thermocouples were place in the surface of the heated cell (*S*), in front (*F*), in the right side (*RS*), in the left side (*LS*) and allow the heated cell (*I*), in the inner part of the tube. In the surface of the heated cell was used an Ômega SA1XL-T-72 thermocouple and in the other points was used a 5TC-GG-K-20-72 thermocouple. The thermocouples were connected to a Novus FieldLogger module, a device that transfers the temperature data to a computer by a USB cable.

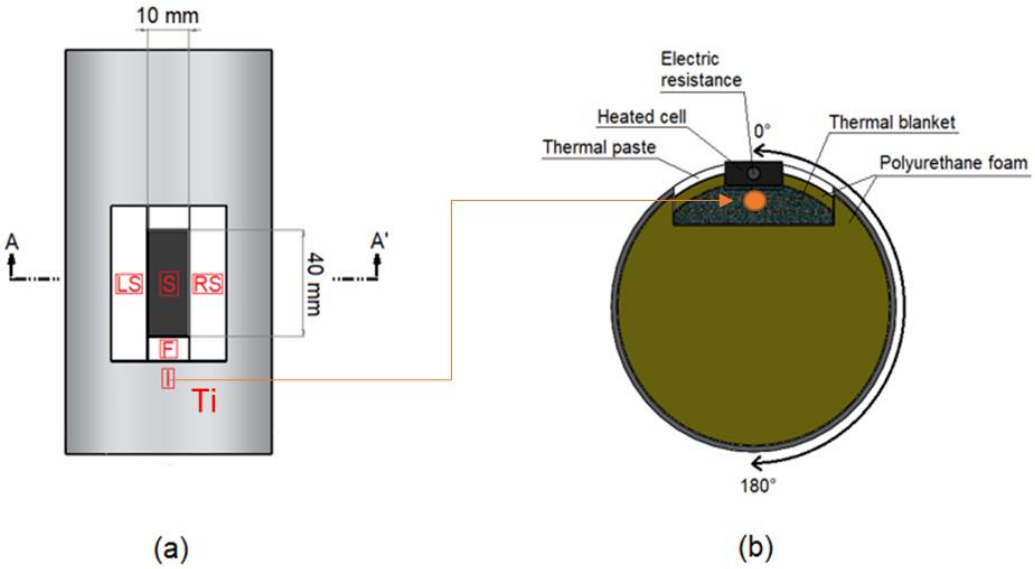


Figure 2. Heated cell. (a) Superior view. (b) Cross section.

The heat transfer was verified by calculating the Nusselt number, according eq. (4), $Nu_{Dh}$ was determined based on the hydraulic diameter, $D_h$ = 0.087 *m.* As a heated source was employed one cartridge resistance housed by a aluminum metal piece. The electrical source Minipa was responsible for heat such resistance at a determined voltage and current (V and I). The heated cell was powered by the electrical source with $q_f$ = 1 *W*. In order to find the convective heat transfer coefficient, first, was necessary to make some considerations about the heat distribution near the heated cell. After some no-flow measurements we observed that the lateral thermocouples changed on 2 °C, while the main one (S), was shown temperature as high as 65°C. At the same time the lower one has changed three times more than those ones placed at the vicinity of the thermocouple (S). Due to this it has been established that the heat transfer was nearly one-dimensional. Part of the flow heat source is transferred to the main flow through the heat transfer convection and the other one is transferred through a conduction mechanism, as shown in Fig. 3.

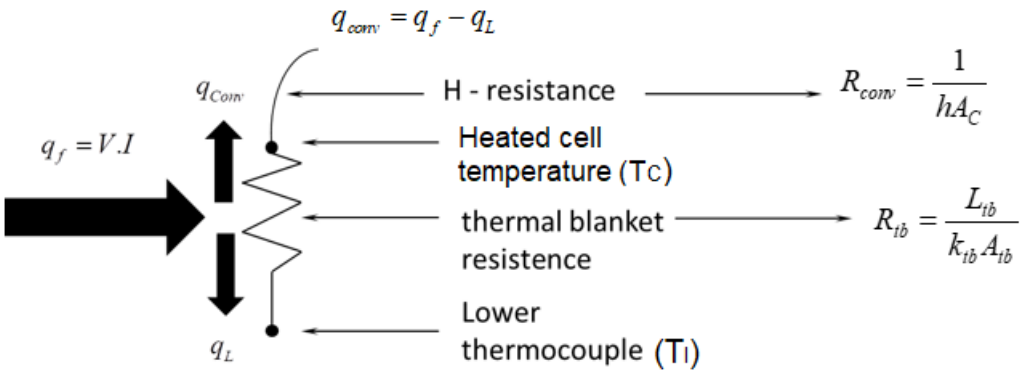


Figure 3. Model for compute the loss heat flux.

Through the schematic thermal resistance model we can compute the convective transfer ($q_{conv}$) between, from the heated cell to the main flow, a follow.

$$q_{conv} = q_f - q_L \tag{1}$$

The conduction heat process between the cell and the thermal blank is ($q_L$), and is given by,

$$q_L = \frac{T_C - T_I}{R_{tb}} \tag{2}$$

$R_{tb}$ is the thermal resistance between the thermal blanket and the heated cell, $k_{tb}$ = 0.04 *w/mk* is the thermal conductivity of the thermal blank, $A_{tb}$ = 0.00165 *m²*, $T_C$ is the heated cell temperature, $T_I$ is the thermal blank surface temperature and $L_{tb}$ = 15 *mm* is the thermal blank thickness.

On the other hand, $R_{conv}$ is the thermal resistance between the heated cell and the air flow. The convective heat transfer was then calculated as,

$$\begin{aligned} q_{conv} &= \frac{T_\phi - T_\infty}{R_{conv}} \\ R_{conv} &= \frac{1}{h_\infty A_C} \end{aligned} \tag{3}$$

In the set of eq. (3) $T_\phi$, $T_\infty$ and $h_\infty$, $A_C$ , are the mean average temperature at each angular position around the cylinder, the mean average flow temperature inside the channel and the calculated heat transfer coefficient at each angular position and the plate's area (0.0004 *m*), respectively. After rescaling the convective heat transfer ($q_{conv}$), it is possible to re-write the convective heat transfer coefficient in terms of Nusselt number, based on the hydraulic-diameter and the air thermal conductivity, $k_{air}$. Afterwards, Nusselt numbers at each azimuthal position, $Nu_\Phi$, were scaled by using the average Nusselt number, $\overline{Nu}_{Dh}$ , as follow in eq. (4).

$$\begin{aligned} Nu_{Dh} &= \frac{hD_h}{k_{air}} \\ Nu_\phi &= \frac{Nu_{Dh}}{\overline{Nu}_{Dh}} \end{aligned} \tag{4}$$

## 3. RESULTS AND DISCUSSION

### 3.1 Average Axial and RMS-fluctuationg Velocities Distributions

The mean average axial velocity and the u-RMS velocity fluctuation were measured to verify the influence of the narrow gap. The figures below show the upper part of the channel, where the gap can be seen. All the velocity points were gathered using the acquisition frequency ($F_a$) and number of points of 1000 *Hz* and 10242, respectively, with the acquisition time ($t_s$) of 10.242 *s*. The number of velocity points measured for the *W*/*D* = 1.05 and *W*/*D* = 1.10 case were 179 and 158, respectively. The Figure 4 shows the isocontours of the average axial velocity, $\overline{U}/U_b$, and the RMS velocity, $u'/U_b$, for the both test sections . The Reynolds number for both experiments are almost the same, being computed with the bulk velocity, $U_b$, the hidraulyc-diameter, $D_h$ and the kinematic viscosity, ν, yielding $Re_{Dh}$ = 40600, for a bulk velocity of 7.24 m/s and 7.44 m/s for *W/D* = 1.05 and 1.10, respectively.

The average axial velocity map, for both geometries showed very similar isocontours in comparison to results presented by Guellouz and Tavoularis (2000a) and Severino (2018). The maximum value for the average axial velocity was 1.8 and the minimum and the minimum, in the gap, was 0.7. In both cases the isoline maps show the isocontours bending towards the narrow gap, most likely due to the strong spanwise velocity component crossing the gap. Despite the gaps difference in terms of width, no relevant differences were found in the mass flow distribution.

However, when the u-RMS is analyzed for both *W/D*-ratios the quantities are notably different. In fig. 4(b) the RMS of the velocity fluctuation is seen the half part in comparison to the Fig. 4 (d). The gap width seems to promote a different mixing in the subchannels. Further, the u-RMS values Figure 4 (d), are in fair agreement with those ones published by Guellouz e Tavoularis (2000a) and Severino (2018), who found such values ranging from 0.14 and 0.06, whereas the maximum and the minimum values found in this work were 0.13 and 0.08, respectively.

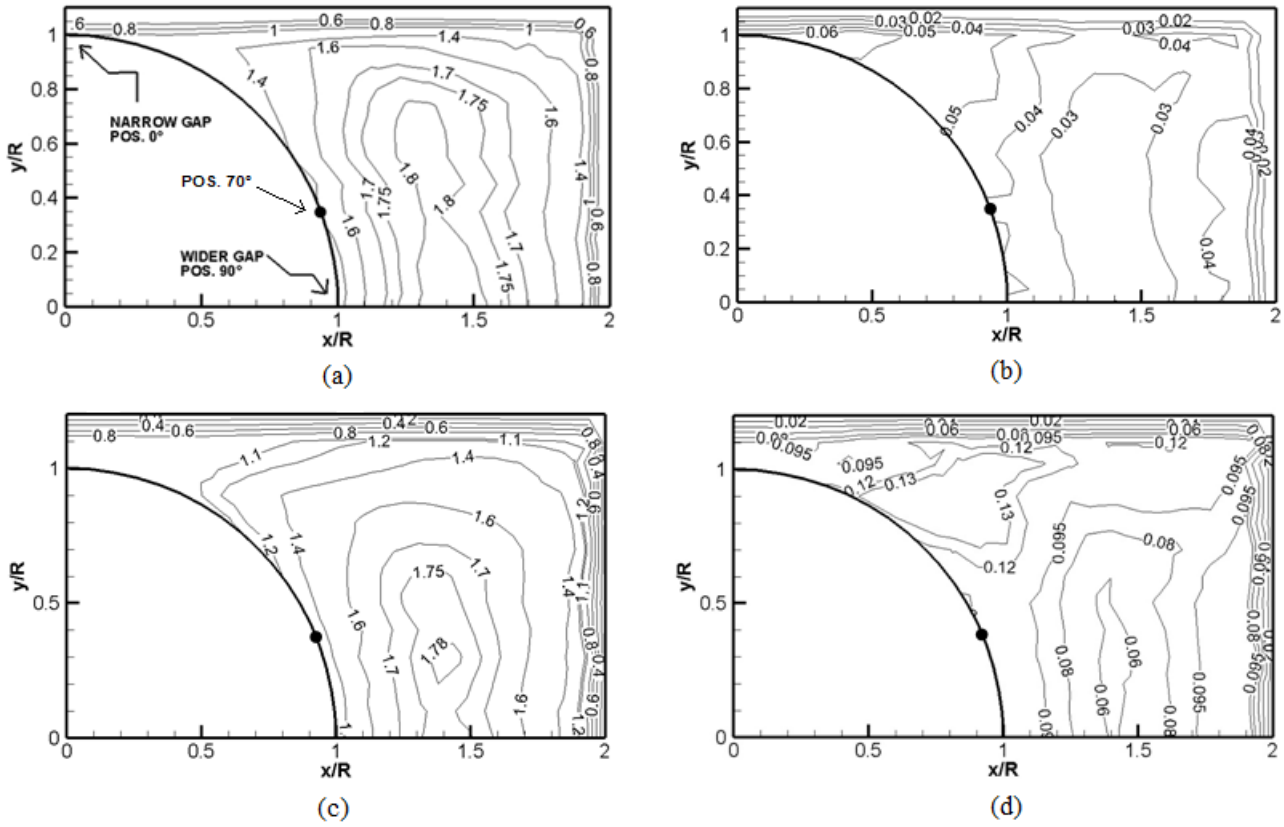


Figure 4. Isocontours of mean axial velocity and u-RMS. a) mean axial velocity for the *W/D* = 1.05. b) mean average u-RMS for the *W/D* = 1.05. c) mean axial velocity for the *W/D* = 1.10. b) mean average u-RMS for the *W/D* = 1.10.

### 3.2 Strouhal Number

In this section the dimensionless velocity spectrum will be presented. This analysis may show the presence of the large-scale structures in the channel, through the presence periodic pattern time-traces velocit. The frequency was dimensionless by the Strouhal number. The Strouhal number was determined by the eq. (5), using the bulk velocity, $U_b$, the tube diameter, *D*. Tavoularis and Chang (2007) calculated the Strouhal number the same way. According to the authors, using the tube diameter to find the Strouhal number is more appropriate, because the hydraulic diameter is mostly determined from parts away from the gap. The spectrum energy was dimensionless by using as scales the bulk velocity and the tube's diameter, according eq. (6). The bandwidth of the spectra is 0.97 Hz.

$$St = \frac{fD}{U_b} \tag{5}$$

$$\psi = \frac{\overline{u'^2}}{DU_b Hz} \tag{6}$$

Figure 5 shows the dimensionless spectra of the fluctuating axial velocities. Both *W/D* = 1.05 and *W/D* = 1.10 dimensionless spectra showed very sharp peaks, showing high energy concentrate in a fundamental frequency. The spectra signals were measured in the line of the 0° position in the channel (Figure 4), the *W/D* = 1.05 spectra was gathered 25 *mm* away from the center of the gap; and *W/D* = 1.10 was measured 30 *mm* away from the center of the gap .This indicates the presence of large coherent structures in the region. Normally, coherent structures are related to narrow regions of the channel, but the results presented in this work suggests that these structures can occurs in regions a little bit far from the gap too. The Strouhal number for the *W/D* = 1.05 and *W/D* = 1.10 were 0.3371 and 0.4202, respectively. These values are very far from the presented by Guellouz and Tavoularis (2000a) and Severino (2018), who found around 0.20. These authors carried out their experiments with a hollow test section, whereas the test section used in this work has both sides closed. It might be an explanation for the discrepancy in the Strouhal number.

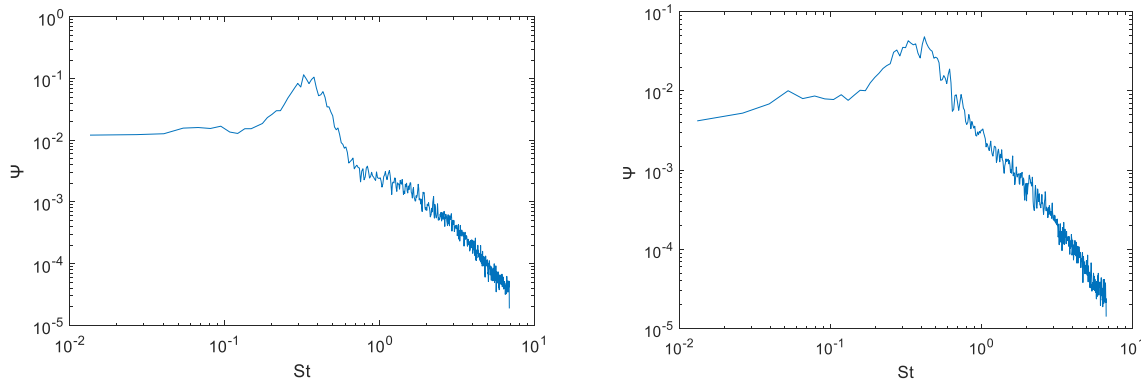


(a) (b)

Figure 5. Dimensionaless spectra of the fluctuating axial velocity. (a) *W/D* = 1.05. (b) *W/D* = 1.10.

### 3.3 Nusselt Number

Figure 6 shows the Nusselt numbers as an azimuthal function. The Nusselt is scaled by the mean average Nusselt number. The local temperature is gathered at each 10 degrees around the rod bundle, and therefore, the local Nusselt is then calculated in form of eq. (4). The position 0° means the center of the narrow gap and 180° is in a wider region.

First of all the lowest values of Nusselt number are in the gap, as we already expected, since the axial velocities are lower, and the viscous effects are the maximum. Departing from the 0° position the local Nusselt values increase azimuthally. Inside the wide subchannel the convective environment is favorable to this kind of heat transfer (higher velocities). For both cases, the minimum and the maximum Nusselt numbers were found the same positions, 0 and 70°, respectively. For *W/D* = 1.05, the maximum Nusselt number was 1.15 and the minimum was 0.84. In the *W/D* = 1.10 configuration, the maximum value was 1.07 and minimum was 0.77. Such numbers are in quite good agreement with those ones published year ago by Chang and Tavoularis (2007) who found Nuϕ ranging from 0.60 in the narrow gap and 1.2, nearby 60°, for the same compound channel characterized as *W/D* = 1.10.

After position 50° the Nusselt variation difference between both channels start to increase, reaching the highest value at about 70° for both gaps. The tiniest gap shows the highest Nusselt variation at 70°, after reaching Nuϕ ~ 1.20, decreasing for further azimuthal positions. On the other hand, after reaching its highest value the value, Nuϕ ~ 1.0 in *W/D* = 1.10, the Nusselt values are almost constant in contrast to the behavior stressed in the tiniest gap, which stress a Nusselt decreasing towards the higher azimuthal positions.

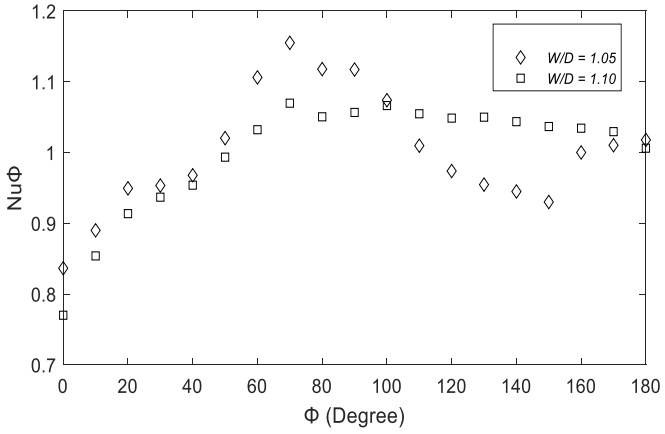


Figure 6. Nusselt number distribution in terms of azimuthal position.

After careful observation we realized that the main heat transfer mechanism seems to be promoted much more by the high axial velocity than its fluctuations. At 70° position both velocity isocontour maps stressed high azimuthal velocities in contrast with low u-RMS values (those supposed to be the additional source of heat diffusion). On the other hand, even stressing the highest u-RMS values, the gap region did not show high heat transfer convective

coefficients. Such result seems to mean that the Nusselt number increasement is more associated to the high axial velocities than to the influence of the coherent structures.

## 4. CONCLUSION

In this work, it was assessed experimentally the influence of the turbulent coherent structures in the convective heat transfer in a compound channel. The experiments were carried out in a rectangular channel containing a single rod bundle in the core. It was possible to analyse the heat transfer by coupling a heat cell in the rod bundle. In this sense, it was determined the Average axial and RMS-fluctuationg velocities; the Strouhal number and the Nusselt number.

The average axial velocity showed similar isocontours with the presented by Guellouz and Tavoularis (2000a) and Severino (2018). However, the lower velocities, in the gap are in relatively good agreement. The maximum value of the average axial velocity for the *W/D* = 1.10 is a little lower than the maximum value of the average axial velocity for the configuration *W/D* = 1.05, something similar is found by Severino (2018). The RMS results, for the *W/D* = 1.10 case, are near to the showed by the authors above.

The spectra for *W/D* = 1.05 and *W/D* = 1.10 showed very pronounced peaks with a fundamental frequency at distinct Strouhal numbers in comparison to other authors. The Strouhal numbers found in this work are 0.3371 and 0.4202 for *W/D* = 1.05 and *W/D* = 1.10, respectively. These values are far from the found by Guellouz and Tavoularis (2000a) and Severino (2018), which was about 0.20. These authors used a hollow test section and the test section used in the present work is closed in both sides. This can explain the differences in the Strouhal number and deserves more observations.

It was determined the Nusselt number distribution over the heated cell, in each 10°, up to 180°. The minimum value for *W/D* = 1.05 and *W/D* = 1.10 were found in the narrow gap, whereas the maximum was found far from the gap, at about 70°. This local is the widest region of the channel and the location of the highest axial velocities. Therefore, in the channel's cross section, the Nusselt number showed to be directly related to the axial velocity, much more than the highest u-RMS values encountered at the gap region.

In terms of the qualitative and quantitative data, our results seems to be in good agreement with the previous results presented in the literature, also enabling the heat cell and the methodology used for performing the measurements and calculations for further analysis.

## 5. ACKNOWLEDGEMENTS

Fábio Matos Kayser would like to thank the Coordenação de Aperfeiçoamento de Pessoal de Nível Superior – Brasil (CAPES) – Finance Code 001 and FAPDF through the research project nº 0193.001.356/2016 (FAPDF) for supporting me during this research.

Jalusa Ferrari and Alexandre de Melo thank to FAPDF for supporting them with fellowships during the work through the research project n° 0193.001.356/2016.

Jhon Nero Vaz Goulart would like to thank to CNPQ and FAPDF for supporting him with a financial aid through the research projects nº 408869/2016-0 (CNPQ), 0193.001.158/2015 (FAPDF) and 0193.001.356/2016 (FAPDF).

Alexandre Alencar de Melo would like to thank FAPDF for supporting him during this research through the research project nº 0193.001.356/2016 (FAPDF).

## 6. REFERENCES

Candela, D. S., Gomes,. T. F., Goulart, J. N. V. and Anflor, C. T. M., 2020. "Numeric simulation of turbulent flow in an eccentric channel". *European Journal of Mechanics / B Fluids*, Vol. 83, pp. 86–98.

Chang, D. and Tavoularis, S., 2007. "Simulation of turbulence, heat transfer and mixing across gaps beetween rod-bundles sub-channels". *Nuclear Engineering and Design*, pp. 109-123.

Goulart, J. N. V., Wissink, J.G., Wrobel, L.C., 2016. "Numerical of turbulent flow in a channel small slot". *Int. Journal of Heat and Fluid Flow*, pp. 343–354.

Guellouz M.S. and Tavoularis S., 1992. "Heat transfer in rod bundle subchannels with varying rod-wall proximity". *Nuclear Engineering and Design.*, pp. 351–366

Guellouz, M. S., 1998. *Turbulent flow and heat transfer in rod bundles*. Ph.D. thesis, University of Ottawa, Ottawa, Canada.

Guellouz, M.S. and Tavoularis, S., 2000a. "The structure of the turbulent flow in a rectangular channel conteining a single rod-Part 1: Reynolds-Average measurements". *Exp Thermal and Fluid Science*, Vol. 23, pp. 59-73

Melo, T., Goulart, J. N. V., Anflor, C. T., Santos, E., 2017. "Experimental investigation of the velocity time-traces of the turbulent flow in a rectangular channel with a lateral slot". *European Journal of Mechanics-B/Fluids*, Vol. 62, pp. 130–138.

Severino, H. A. M., Melo, T., Goulart, J. N. V. "Hot wire anemometry and numerical simulation applied to the investigation fo the turbulence in a gap flow". *6th European Conference on Computational Mechanics (ECCM 6) and 7th European Conference on Computational Fluid Dynamics (ECFD 7) - ECCOMAS 2018.* Glasgow, UK.

Tavoularis, S. and Chang, D. "Inter-subchannel mixing across very narrow gaps in rod-bundles". *15th International Conference on Nuclear Engineering* – 2007. Nagoya, Japan.

## 7. RESPONSIBILITY NOTICE

The authors are the only responsible for the printed material included in this paper.